University of Thessaly

Department of Mechanical Engineering

Simulation of the strain induced precipitation of Nb carbon nitrides in HSLA steels

Προσομοίωση καθίζησης από νιτρίδια άνθρακα Nb σε χάλυβες υψηλής αντοχής και χαμηλής κραμάτωσης

By Dimitrios N. Mamouchas

Submitted to the Department of Mechanical Engineering in February 2025 in partial fulfillment of the requirements for the degree of Mechanical Engineer.

Thesis Committee

Gregory N. Haidemenopoulos

Helen M. Kamoutsi

Anna D. Zervaki

Abstract

The development of High Strength Low Alloy (HSLA) steels, renowned for their superior mechanical properties, hinges on a profound understanding of strain-induced precipitation phenomena. This study investigates the precipitation kinetics of niobium (Nb) carbonitrides, pivotal for optimizing the thermomechanical control processes (TMCP) used in HSLA steel production. Utilizing the TC-PRISMA software, simulations were performed to analyze the effects of material parameters such as interfacial energy, nucleation sites, and mobility factors on nucleation, growth, and coarsening. Parametric analyses on Fe-C systems provided critical insights into the interaction of material parameters, revealing the influence of diffusivity, activation energy, and solvus line characteristics. Subsequent simulations on a HSLA steel demonstrated the sensitivity of Nb precipitation kinetics to TMCP parameters. Key findings highlighted the impact of phase competition, particularly between Nb and Ti-rich phases, on the evolution of particle size distribution and volume fraction.

Table of Contents

List of Figures

List of Tables

1. Introduction

The ongoing advancements in materials science necessitate the development and study of advanced high-strength steels (AHSS), such as High Strength Low Alloy (HSLA) steels. They are a type of alloy steel with low carbon content (0.05-0.25 wt%) which boast improved mechanical properties such as strength, weldability, toughness and atmospheric corrosion resistance compared to common carbon steel. Due to their excellent mechanical properties, HSLA steel has been employed in a wide range of applications such as oil and gas pipeline [1], [10], heavy-duty highway and off-road vehicles, industrial equipment, offshore structures and bridges. The improved properties of HSLA steels are a result of a plethora of alloying elements in small quantities, such as Nitrogen, Titanium, Copper, Niobium, Vanadium, Nickel, as well as the by the appropriate Thermomechanical Control Process (TMCP) [2],[3] applied during manufacturing. The presence of these alloying elements creates carbonitrides in the material, which in turn during the TMCP, hinder the grain growth of the microstructure, resulting in a fine grain structure and they provide precipitation hardening at the same time. Therefore, the control and understanding of the precipitation of these carbonitrides is a prerequisite for the design and development of HSLA steels.

Thermomechanical Control Process (TMCP), which consists of controlled hot-rolling and controlled cooling has a significant role in the development of HSLA steels. During the multipass hot-rolling, the main phenomena which control the microstructure evolution is the austenite recrystallization and the strain-induced precipitation of carbonitrides [4],[8],[12] , especially of Nb. The key to process design is to control the interaction of the phenomena. After deformation in pass, static recrystallization takes place resulting in a refined structure. Strain-induced precipitation of Nb carbonitrides is also possible to occur, depending on the processing parameters. The Nb precipitates exert a Zener Pining force at the grain boundaries, impeding in this way the grain growth. A fine distribution on Nb precipitates is required to inhibit grain growth and ensure precipitation hardening. Thus, the study of Nb particle growth and coarsening is necessary.

One of the very first studies on particle growth and coarsening was from Lifshitz and Slyozov [5], who aimed to predict the particle distribution. Kampmann and Wagner were the first to introduce a robust arithmetical model to simulate the simultaneous process of nucleation, growth and coarsening; namely the Kampmann-Wagner Numerical (KWN) model [6]. They based their work on the approach of Langer and Schwarz (LS) and the modified version of it (MLS). One tool designed to help with the alloy design is the software Thermocalc-PRISMA [7], which simulates the precipitation process and gives data for the radius, size distribution and composition of the precipitates. Through multiple iterations we can reverse the simulation process and can produce a thermal profile for a heating process for the material given the precipitate properties as input. TC-PRISMA adopts the KWN model to simulate the connected processes of nucleation, growth and coarsening of precipitates.

In this study, the TC-PRISMA software was adopted to investigate the growth and coarsening of Nb particles. Initially, the TC-PRISMA was employed to understand the effect of material parameters such as interfacial energy, mobility and number of nucleation sites on the precipitation kinetics, for the case of plain Fe-C steel during cementite precipitation at an isothermal temperature. After understanding the effect of material parameter, the software

was employed for the description of strain-induced precipitation kinetics of Nb carbonitrides for the case of a HSLA steel, during isothermal holding after deformation in a pass. The material parameters were calibrated based on experimental observations of a HSLA steels reported by S. Vervynckt et al. [8]. The aim of this work is to understand the strain-induced precipitation kinetics of Nb carbonitrides and the effect of processing parameters on the nucleation, growth and coarsening of Nb particles.

2. Methodology

Simulation Tools

THERMO-CALC

Thermo-Calc [9] is a software and database package for all kinds of phase equilibrium, phase diagram (binary, ternary, multi-component) and phase transformation calculations and thermodynamic assessments. It has been developed for complex heterogeneous interaction systems with strongly non-ideal solution phases and can be applied to any thermodynamic system in the fields of chemistry, metallurgy, material science, alloy development, geochemistry, semiconductors etc. depending on the kind of database it is connected to. The thermodynamic databases are produced through critical assessment and systematic evaluation of experimental and theoretical data, following the well-established CALPHAD technique. Thermo-Calc allows explicit conditions to be set on individual phase compositions or configuration for example, activities and chemical potentials of the components, volumes, enthalpies, entropies. In this work, the critical temperatures will by calculated by Thermo-Calc using the TCEF6 database for ferrous alloys.

TC-PRISMA

The TC-PRISMA software is a general computational tool for simulating kinetics of diffusion controlled multi-particle precipitation processes in multi-component and multi-phase alloy systems. Precipitation, formation of particles of a second phase or second phases from a supersaturated solid solution matrix phase, is a solid-state phase transformation process that has been exploited to improve the strength and toughness of various structural alloys. This process is thermochemically driven and fully governed by system (bulk and interface) thermodynamics and kinetics. Typically, a precipitation process has three distinctive stages: nucleation, growth, and coarsening. However, under certain conditions, they could happen also at the same time. With TC-PRISMA, the kinetics of concurrent nucleation, growth, and coarsening can be simulated by calculating the evolution of the probability distribution of the particle number densities, usually called particle size distribution (PSD). The simulation results can be used to understand and guide how to obtain desirable precipitates with certain PSD or to avoid undesirable precipitations during heat treatments of alloys such as aging and tempering. TC-PRISMA is directly integrated with Thermo-Calc and DICTRA, which are CALPHAD based computer programs for calculating phase equilibrium and diffusion-controlled phase transformation in multicomponent systems and have a wide spectrum of accompanying thermodynamic and kinetic databases. However, a few other physical properties, such as interfacial energy and volume, are needed in precipitation models

implemented in TC-PRISMA. These additional physical parameters can be obtained by experiments or other estimation models or first principles calculations. In this work the thermodynamic database TCFE6 and the kinetic database MOBFE2 for steels were employed for the simulations.

It has two modes of operation, CALPHAD based calculation and user-defined binary calculation. The steps for performing a simulation are:

- Defining the system
- Setting the conditions
- Setting the nucleation properties
- Setting the parameters

PRISMA will run the simulation and export a series of data files which can be used to plot diagrams for the nucleation rate, particle size distribution, number density, mean and critical radius, volume fraction, matrix and precipitate compositions.

Thermomechanical Control Process of HSLA (TMCP) and phenomena

The thermomechanical control process of HSLA steels begins with heating in the austenite region. As long as the hot rolling is performed above the temperature of no recrystallization T_{NRX}, the austenite grains remain equiaxed due to static recrystallization after deformation. Addition of alloying elements such as niobium in solid solution impedes recrystallization. When the deformation occurs below T_{NRX}, an austenite pancake structure is formed and the density of the grain boundaries increases. Thus, during cooling in the α+γ region, the high nucleation rate of ferrite in the austenite grain boundaries results in a finer grain size microstructure. Furthermore, the precipitation of carbonitrides inhibits the migration of the grain boundaries. Depending on the cooling rate, formation of bainite is possible. The final microstructure consists of ultrafine ferrite and sometimes of different types of bainite. The mechanical properties depend on the weight fraction and shape of the phases, the fine spatial particle distribution and the grain size. Using the thermomechanical control process a wide range of HSLA steels for pipeline applications is produced.

Principles of Kampmann-Wagner Numerical (KWN) model

The Kampmann-Wagner Numerical (KWN) model is a robust framework used to simulate the nucleation, growth, and coarsening of precipitates in materials. This model is particularly useful for understanding the precipitation kinetics in high-strength low-alloy (HSLA) steels. The KWN model is based on the following principles:

Nucleation

Nucleation is the initial stage where small clusters of atoms form within the supersaturated matrix. The KWN model calculates the nucleation rate, which is influenced by factors such as supersaturation, temperature, and the availability of nucleation sites. The critical radius, which is the size at which a nucleus becomes stable and can grow rather than dissolve, is a key parameter in this stage. The nucleation rate (J_s) can be expressed as:

$$J_s = Z\beta^* N_0 \exp\left(\frac{-\Delta G^*}{kT}\right)$$

where:

- (Z) is the Zeldovich factor,
- (β^*) is the rate at which atoms attach to the nucleus,
- (N_0) is the number of potential nucleation sites,
- (ΔG^*) is the critical free energy barrier for nucleation,
- (k) is the Boltzmann constant,
- (T) is the absolute temperature.

Growth

Once nucleated, the precipitates grow by the diffusion of solute atoms to the precipitate-matrix interface. The growth rate is controlled by the diffusion coefficient of the solute atoms and the interface mobility.

Coarsening (Ostwald Ripening)

Over time, larger precipitates grow at the expense of smaller ones, a process known as coarsening or Ostwald ripening. This process is driven by the reduction in total interfacial energy. The Lifshitz-Slyozov-Wagner (LSW) theory is often used to describe the kinetics of coarsening. According to LSW theory, the average radius $\bar{r}$ of the precipitates increases with time (t) as:

$$\bar{r}^3 - \bar{r_0}^3 = Kt$$

where:

- ($\bar{r_0}$) is the initial average radius,
- (K) is a coarsening rate constant that depends on the diffusion coefficient and the interfacial energy.

Particle Size Distribution (PSD)

The KWN model tracks the evolution of the particle size distribution (PSD) over time. This involves calculating the number density of particles as a function of size, which provides insights into the kinetics of nucleation, growth, and coarsening. The PSD is typically represented by a probability distribution function.

Thermodynamic and Kinetic Inputs

The KWN model relies on accurate thermodynamic and kinetic data. The CALPHAD (Calculation of Phase Diagrams) approach is often used to provide thermodynamic data, while kinetic parameters such as diffusion coefficients, interfacial energies, and nucleation site densities are critical inputs for the model.

Simulation of Concurrent Processes

One of the strengths of the KWN model is its ability to simulate the concurrent processes of nucleation, growth, and coarsening. This comprehensive approach allows for a detailed understanding of the precipitation kinetics in complex alloy systems.

By incorporating these principles, the KWN model provides a detailed and accurate simulation of the precipitation processes in HSLA steels, aiding in the optimization of thermomechanical control processes to achieve desired microstructures and mechanical properties.

Parametric analysis and carbonitride precipitation simulation

A comprehensive understanding of the TC-PRISMA software is essential for accurate parametric analysis and simulation. For that purpose, a simple system was chosen as a basis for a parametric analysis using the software. The chosen system is an isothermal precipitation of Cementite in a ferritic steel Fe-C (7E-4 mole fraction, 0.01505 wt%) at 270 °C for 1E5 seconds. All the available inputs were regarded as variables for the parametric analysis and were examined separately.

Calphad Base Simulation	**User Defined Binary Simulation**
Nucleation Sites, Dislocation Density	Nucleation Sites, Dislocation Density
Mobility	Diffusivity
Phase Energy Addition	Solvus Line
Interfacial Energy	Interfacial Energy
Phase Boundary Mobility	

Table 1: Variables of parametric analysis.

The precipitation of Nb carbon nitrides is simulated in a HSLA steel with composition used by Vervynckt et al. so as the software can be calibrated using the experimental data they provide. The thermal process the steel goes through starts with reheating at 1250°C for 5 minutes, cooling at a rate of -30°C/s and it goes through a first deformation pass at 1000°C. Average diameter, precipitated Nb(wt%) and volume fraction of the precipitate are provided for different times after the deformation pass (1s, 10s, 30s, 100s, 500s, 1000s, 5000s) which will be used as data to calibrate the software with.

Using Thermo-calc at 1000°C, the full steel composition reveals three phases: γ-Fe (FCC) as the matrix, and two precipitant phases, FCC#2 and FCC#3, with one being rich in Niobium and the other in Titanium. A limitation encountered when inputting the full steel composition into PRISMA is its inability to differentiate between the two phases, leading to the simulation of the Ti-rich phase. To address this, the Titanium element was removed from the composition, allowing the software to simulate the desired precipitation process.

	C	Mn	Si	Al	Nb	Ti	N
C-Nb Reference	0.02	1.5	0.26	0.067	0.16	80ppm	20ppm
PRISMA composition	0.02	1.5	0.26	0.067	0.16	-	20ppm

Table 2: Selection of material composition

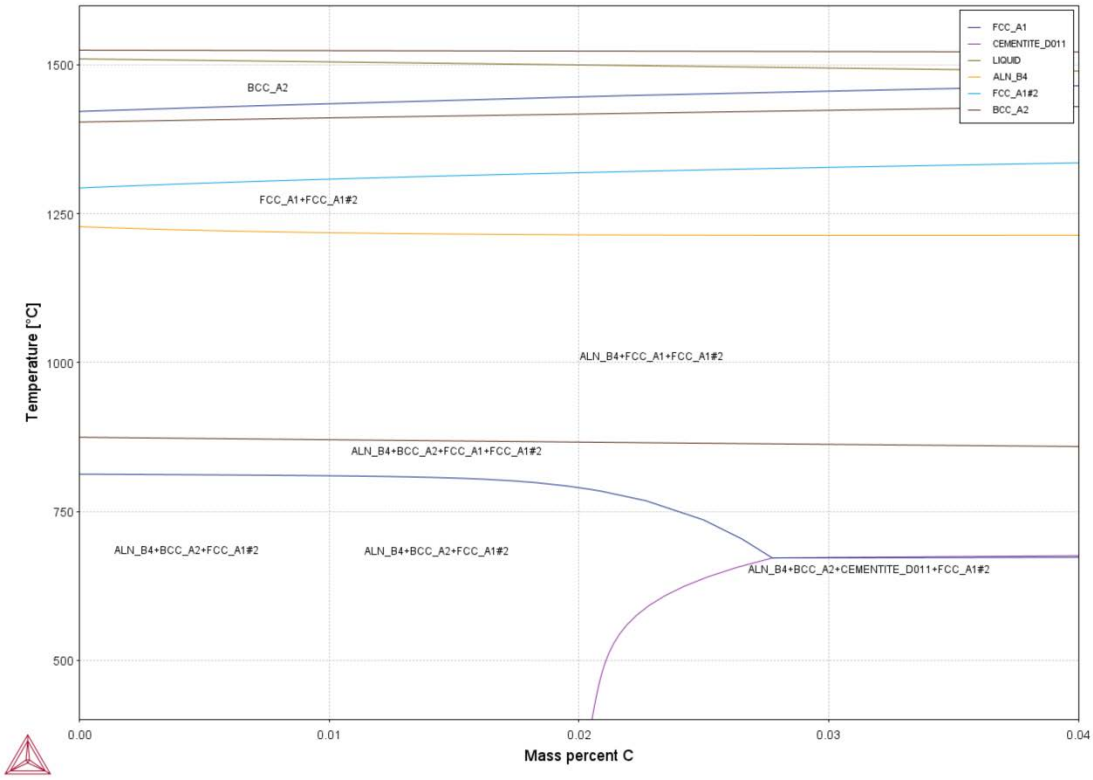

Figure 1: Phase diagram of reference steel. FCC_A1#2 is the rich in Nb precipitate phase.

3. Results and Discussion

The accuracy of the output relies on properly understanding the influence the parameters have on the calculations. For this purpose, a parametric analysis was conducted on a given example of a Carbon Iron alloy with Cementite as the only precipitant.

The following inputs are kept as constant

- Composition set at C (0.07% mole fraction)
- Temperature profile set at 270 °C for 1E5 (seconds)

The first parameter examined is the effect of nucleation sites on nucleation, growth, and coarsening during the simulations. It is also crucial to understand how the position of nucleation sites influences the kinetics of precipitation. The program interface requires either the dislocation density or the number of nucleation sites as input. The analysis was conducted by varying both values, followed by further simulations to identify the effects of Grain Aspect Ratio and Grain Size on precipitation.

A high number of nucleation sites or a high dislocation density facilitates the precipitation process. The impact of the number and position of nucleation sites is illustrated in Figure 2. It is observed that increasing the number of nucleation sites diminishes the influence of individual sites. Conversely, reducing the number of nucleation sites shows that nucleation in the bulk material, grain corners, and grain edges follows the same pattern, resulting in

identical plot lines in the compiled results. Further analysis indicates that dislocations act as slower nucleation sites compared to the bulk material, with grain boundaries being even slower.

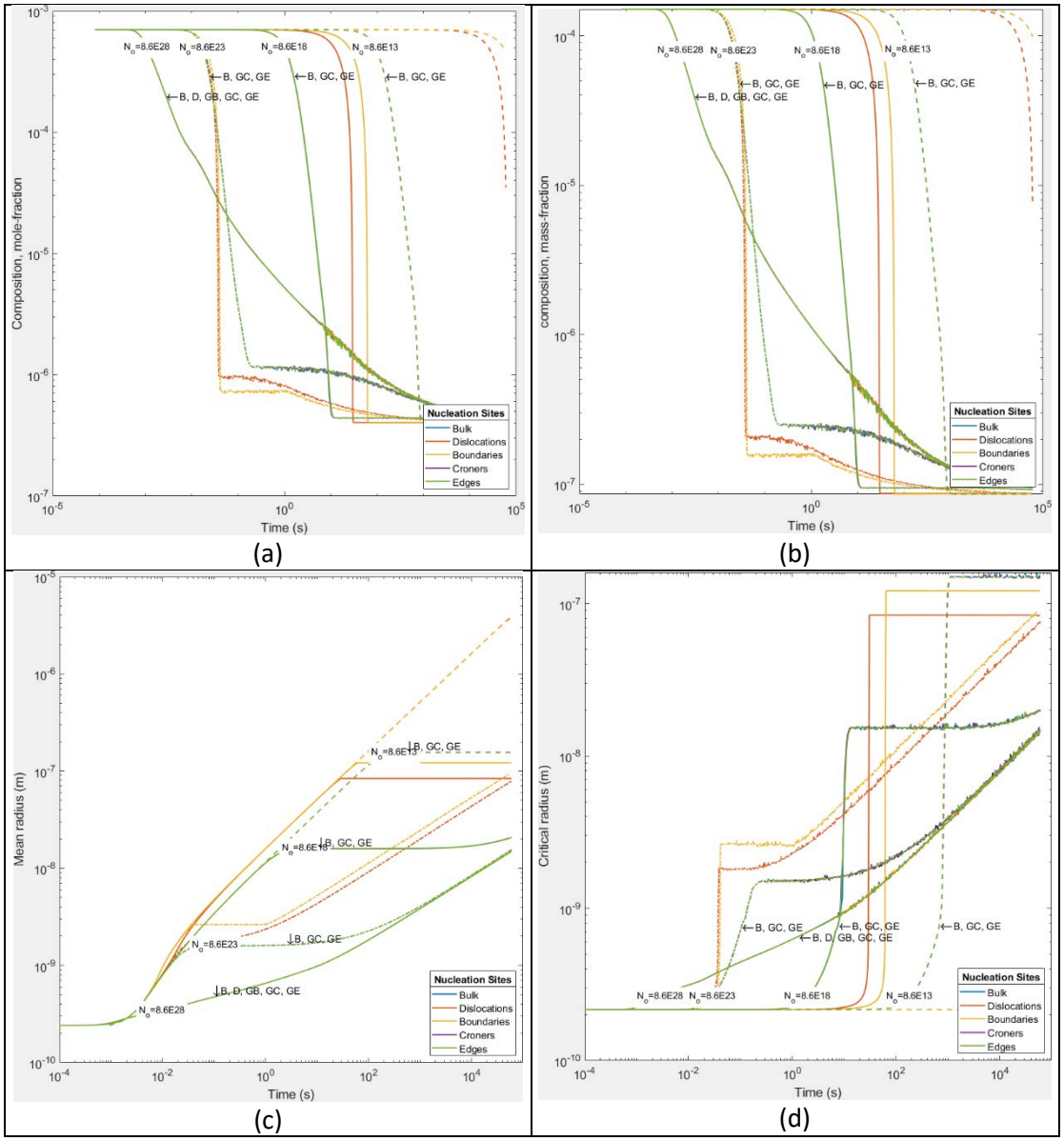

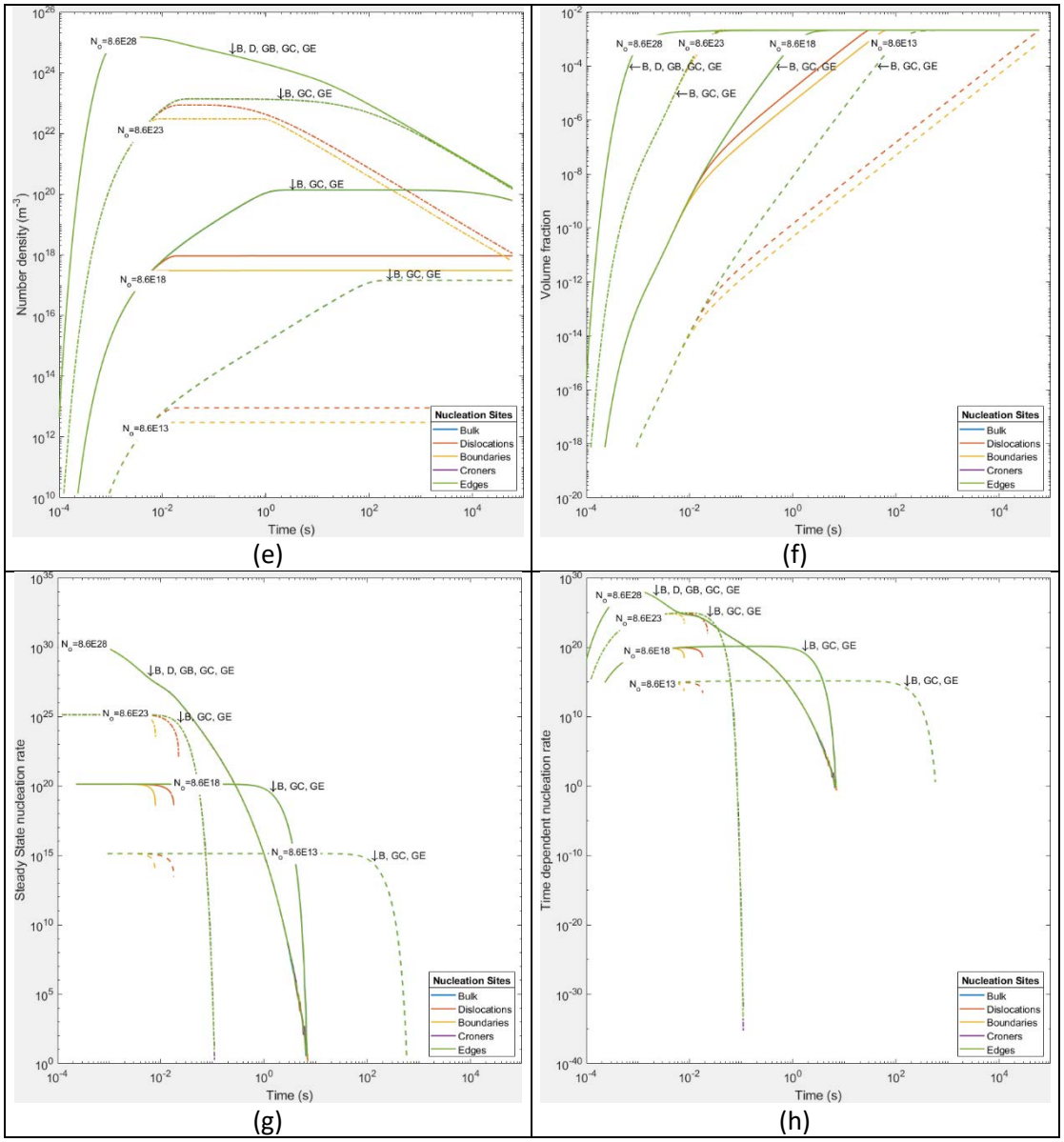

Figure 2: Effect of Nucleation Sites to (a) composition mole-fraction vs. time, (b) composition mass-fraction vs. time, (c) mean radius vs. time, (d) critical radius vs. time, (e) number density vs. time, (f) volume fraction vs. time, (g) steady state nucleation rate vs. time, (h) time dependent nucleation rate vs. time.

CALPHAD based calculation mode

The following parameters were adjusted for the analysis:

Parameter	Range
Mobility Enhancement Prefactor	0.01 ~ 5
Mobility Enhancement Activation Energy	1e-5 ~ 7.5e4
σ Interfacial Energy	0.1 ~ 0.4
Phase Boundary Mobility	1e-10 ~ 1e5
Phase Energy Addition	-1000 ~ 10000

Table 3: Calphad based parameters analyzed.

Mobility Enhancement Prefactor

A prefactor that applies to the mobility from the CALPHAD database. It can be used to artificially accelerate the precipitation.

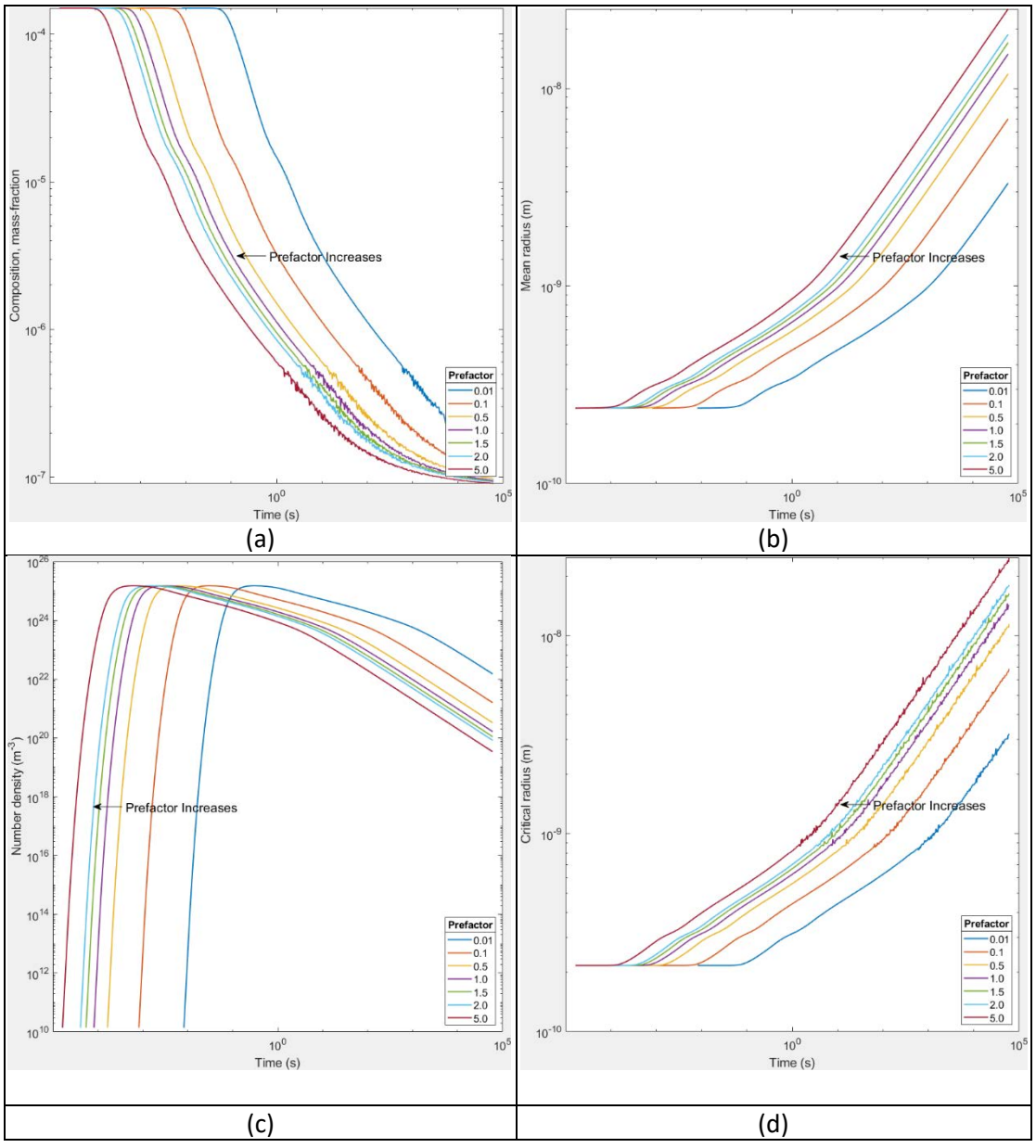

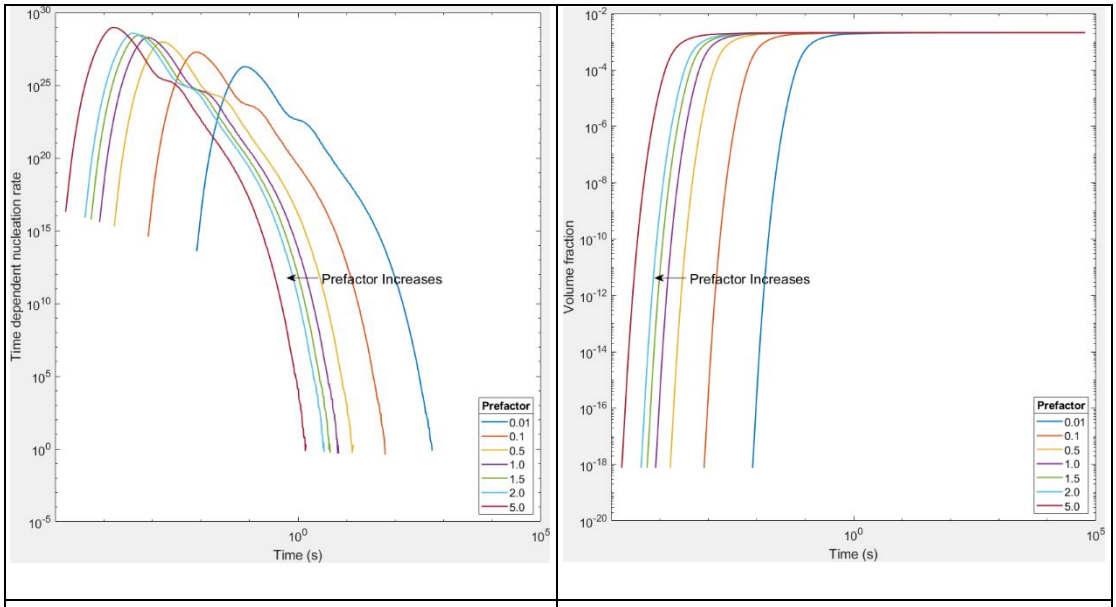

(e) (f)

Figure 3: Effect of mobility enhancement prefactor for (a) composition mass-fraction vs. time, (b) mean radius vs. time, (c) number density vs. time, (d) critical radius vs. time, (e) time dependent nucleation rate vs. time, (f) volume fraction vs. time.

An increase to the mobility enhancement prefactor Mo leads to a faster start of the nucleation, growth and coarsening processes as can be observed from the data. The calculated values for composition, number density, volume fraction, mean and critical radii appear to be shifted only in the time axis, meaning they don't produce any change in their profile. In contrast the nucleation rate is increased in value as seen from Figure 3,(e). This result mirrors the theory. Increasing the mobility or diffusivity for the precipitate makes the nucleation, growth and coarsening processes easier to take place.

Mobility Enhancement Activation Energy

A value that adds to the activation energy of mobility data from database. This value scales the mobility by a temperature dependent amount, same as mobility enchantment prefactor.

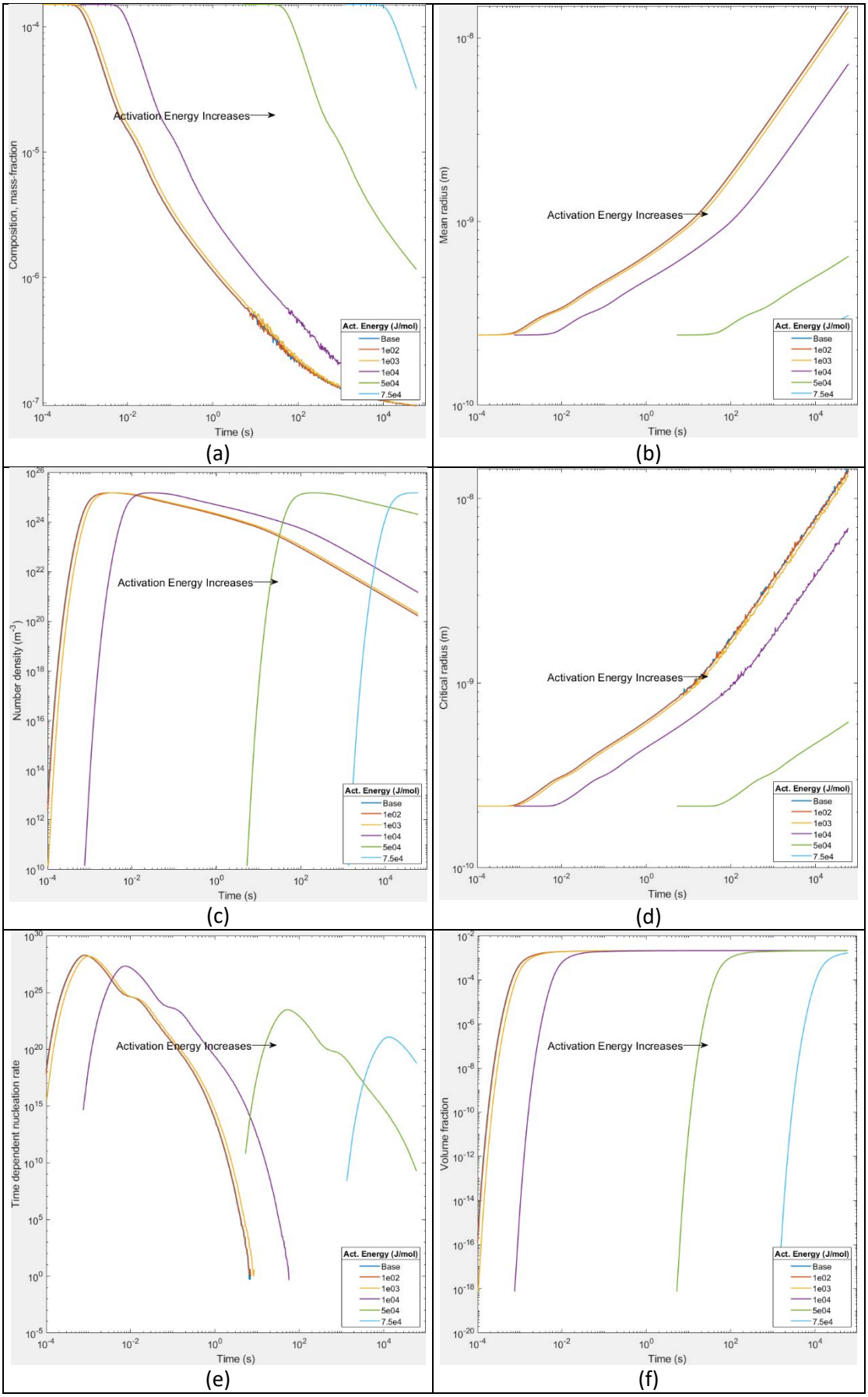

Figure 4: Effect of mobility enhancement activation energy for (a) composition mass-fraction vs. time, (b) mean radius vs. time, (c) number density vs. time, (d) critical radius vs. time, (e) time dependent nucleation rate vs. time, (f) volume fraction vs. time.

The effect of mobility enhancement activation energy E_A(J/mol) is opposite to that of the mobility enhancement prefactor. An increase in activation energy decreases the nucleation rate and delays its onset. The activation energy acts as an energy barrier, making the processes of nucleation, growth, and coarsening slower and more challenging. Notably, the impact of activation energy is exponential compared to the linear effect of the prefactor.

Interfacial Energy

The adjustments applied to the interfacial energy σ (J/m^2) were on a smaller scale compared to other parameters, as its effect on the calculations is of a greater magnitude, as seen from the equation $\Delta G^* = \frac{16\pi\sigma^3}{3\left(\Delta G_m^{\alpha\to\beta} / V_m^{\beta}\right)^2}$, where:

- (ΔG*) is the Gibbs energy of formation of a critical nucleus,
- (σ) is the interfacial energy,
- ($\Delta G_m^{\alpha\to\beta}$) is the molar Gibbs energy change for the formation of the β precipitate and
- (V_m^{β}) is the molar volume of the β precipitate phase.

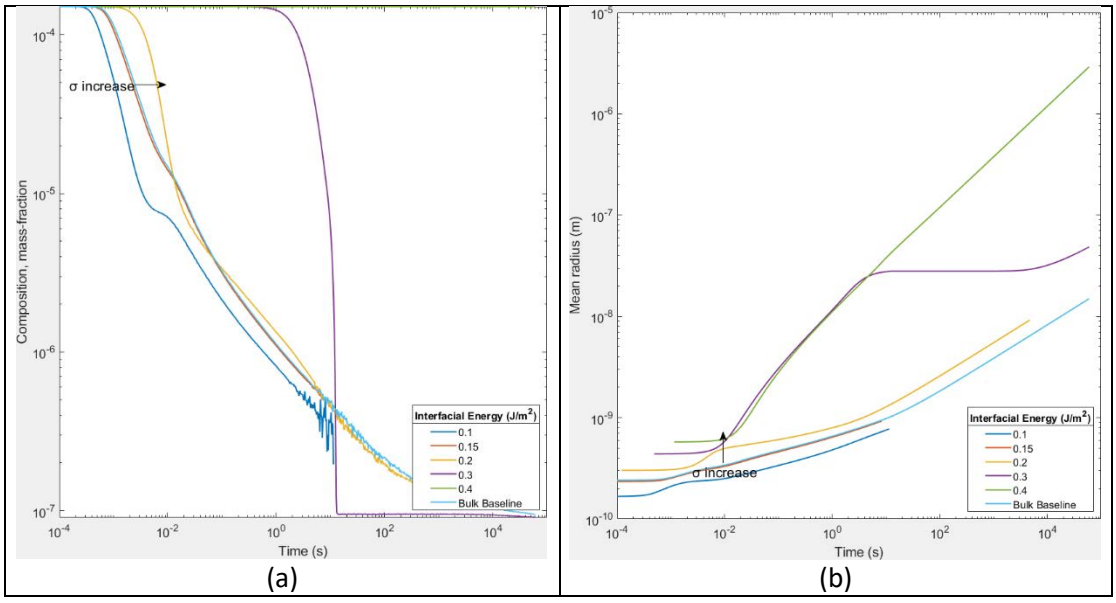

(a) (b)

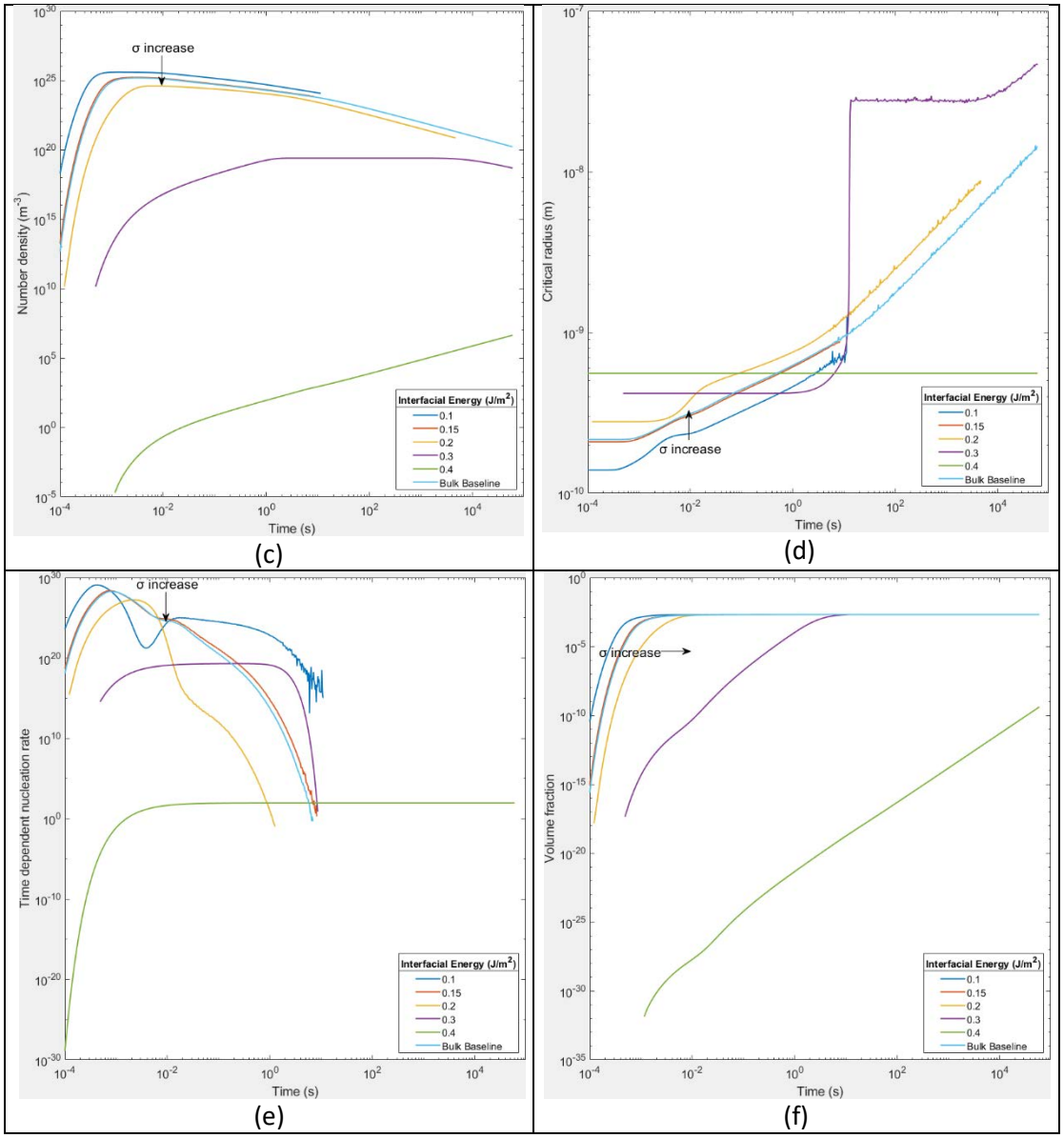

Figure 5: Effect of interfacial energy for (a) composition mass-fraction vs. time, (b) mean radius vs. time, (c) number density vs. time, (d) critical radius vs. time, (e) time dependent nucleation rate vs. time, (f) volume fraction vs. time.

Interfacial energy σ significantly influences the nucleation rate during phase transformations. Higher interfacial energy increases the energy barrier that must be overcome for nucleation to occur, resulting in a larger critical nucleus size. Consequently, this makes nucleation less likely and reduces the nucleation rate. Conversely, lower interfacial energy decreases the energy barrier, facilitating a higher nucleation rate. Thus, interfacial energy acts as a deterrent to nucleation by increasing both the energy barrier and the critical nucleus size, thereby reducing the nucleation rate.

Phase Boundary Mobility

Within the tested range, no changes were observed in the output for this parameter. It appears that this parameter is relevant for precipitation simulations that follow the interface

control model rather than the diffusion control model. In a different system, this parameter would likely produce changes in the output.

Phase Energy Addition

A parameter that directly adds the given value to the Gibbs free energy (ΔG*) from the Calphad database.

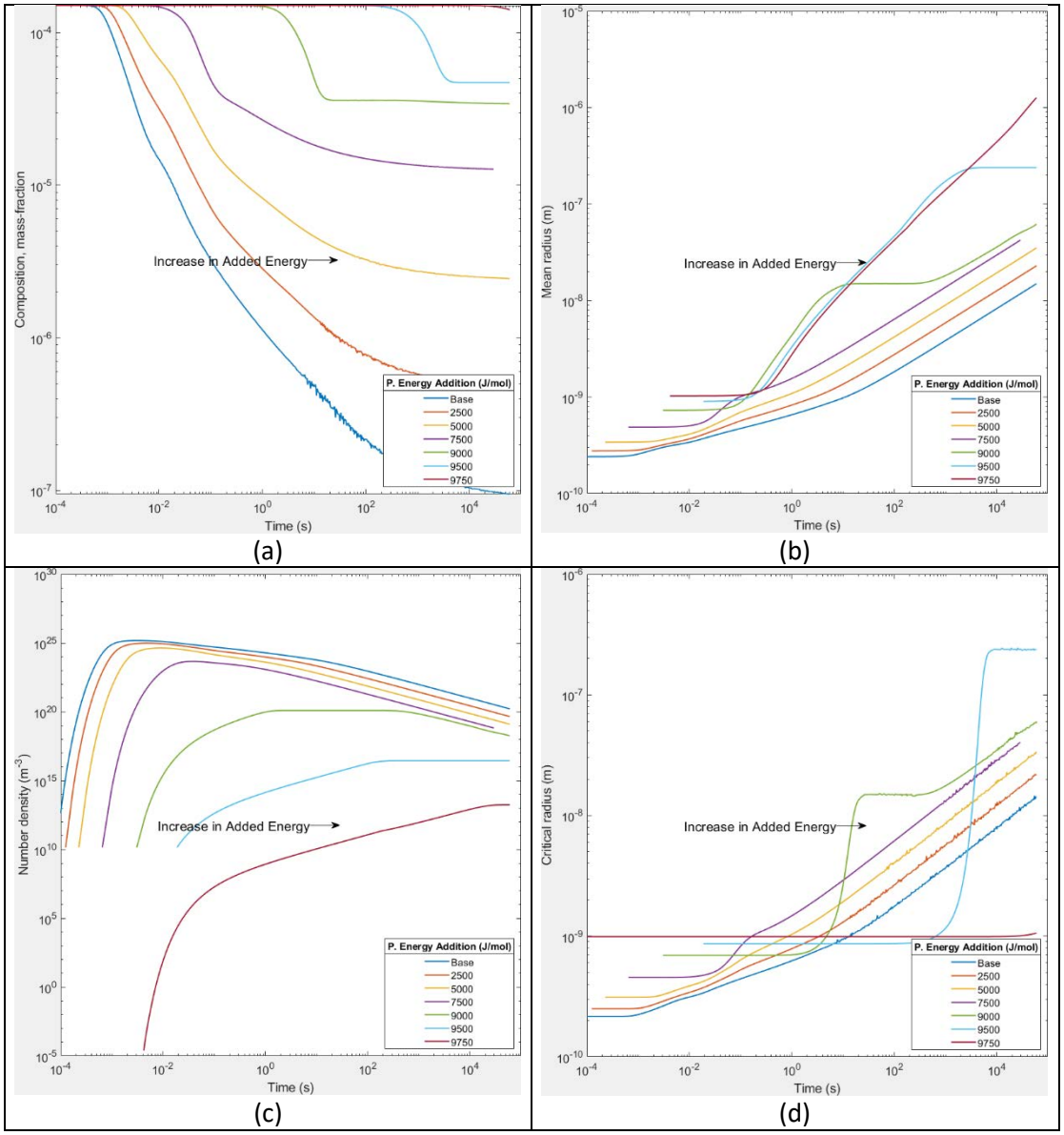

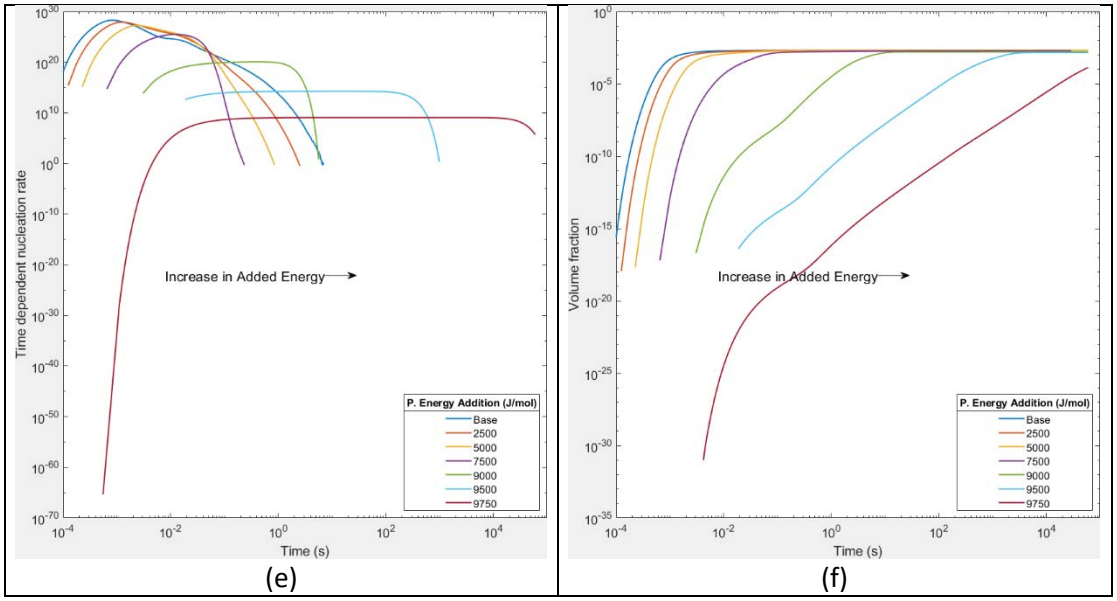

Figure 6: Effect of phase energy addition for (a) composition mass-fraction vs. time, (b) mean radius vs. time, (c) number density vs. time, (d) critical radius vs. time, (e) time dependent nucleation rate vs. time, (f) volume fraction vs. time.

An increase in the Gibbs free energy (ΔG*) significantly impacts the nucleation, growth, and coarsening of Nb carbonitrides in HSLA steels. Higher Gibbs free energy raises the energy barrier for nucleation, thereby reducing the nucleation rate as more energy is required to form stable nuclei. This also results in a larger critical nucleus size, making nucleation less likely. Additionally, the increased energy barrier slows down the growth and coarsening processes, as atoms or molecules need more energy to attach to existing nuclei or precipitates. Consequently, an increase in Gibbs free energy acts as a deterrent to these processes, making them less likely to occur and slower when they do.

User-defined binary calculation mode

The following five parameters were adjusted for the analysis:

Parameter	Range
D_0 Diffusivity Prefactor	6.2e-10 ~ 6.2e-2
E_A Diffusivity Activation Energy	8e1 ~ 12e4
σ Interfacial Energy	0.0174 ~ 2088
Solvus Line Prefactor	1e-1 ~ 1e-5
Solvus Line Activation Energy	

Table 4:User-defined binary based parameters analyzed.

Diffusivity prefactor and activation energy for the matrix and Interfacial energy, Solvus line prefactor and activation energy for the precipitate.

Matrix – Diffusivity Prefactor

The prefactor was adjusted by orders of magnitude to observe its effect on the output. Increasing the prefactor by an order of magnitude resulted in a corresponding increase in both steady-state and time-dependent nucleation rates, while simultaneously decreasing the time

required for nucleation to commence. Conversely, decreasing the prefactor had the opposite effect.

$D = D_0 \exp\left(-\frac{E_A}{RT}\right)$, where:

- (D) is the diffusivity
- (D_0) is the max diffusion coefficient (at infinite temperature)
- (E_A) is the activation energy for diffusion
- (T) is the absolute temperature
- (R) is the universal gas constant.

From the equation $\beta^* = \frac{4\pi r^{*2} X^{\alpha} D}{\alpha^4}$, where:

- (β*) is the rate at which atoms or molecules are attached to the critical nucleus,
- (r*) is the critical radius,
- (X^{α}) is the mole fraction of α component
- (α) is the lattice parameter and
- (D) is the Diffusivity,

It is observed that, indeed, an increase in D leads to an increase to the quantity β^*, which in turn increases the nucleation rates

$J_s = Z\beta^* N_0 \exp\left(\frac{-\Delta G^*}{kT}\right)$ and $J(t) = J_s exp\left(-\frac{\tau}{t}\right)$.

An increase in the diffusivity prefactor results in transformations happening earlier without any other effect in the magnitude of them, as can be seen from the other graphs. In the graphs we can see the matrix composition decreasing at different times and stabilizing at the same value between the different prefactor values. Same behavior is observed in mean and critical radius graphs as well as in the number density and volume fraction of cementite.

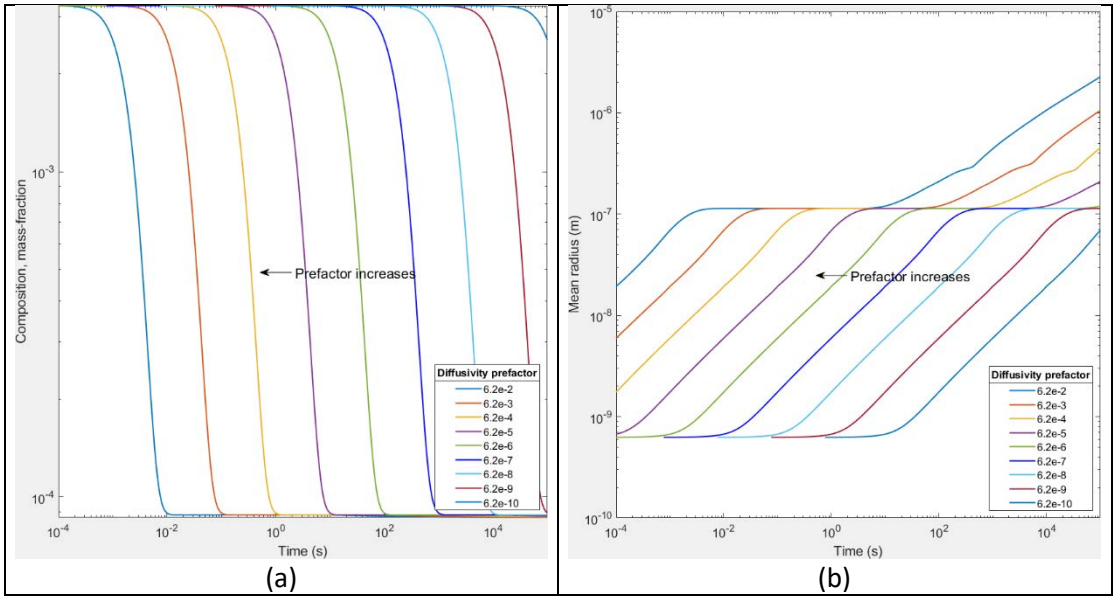

(a) (b)

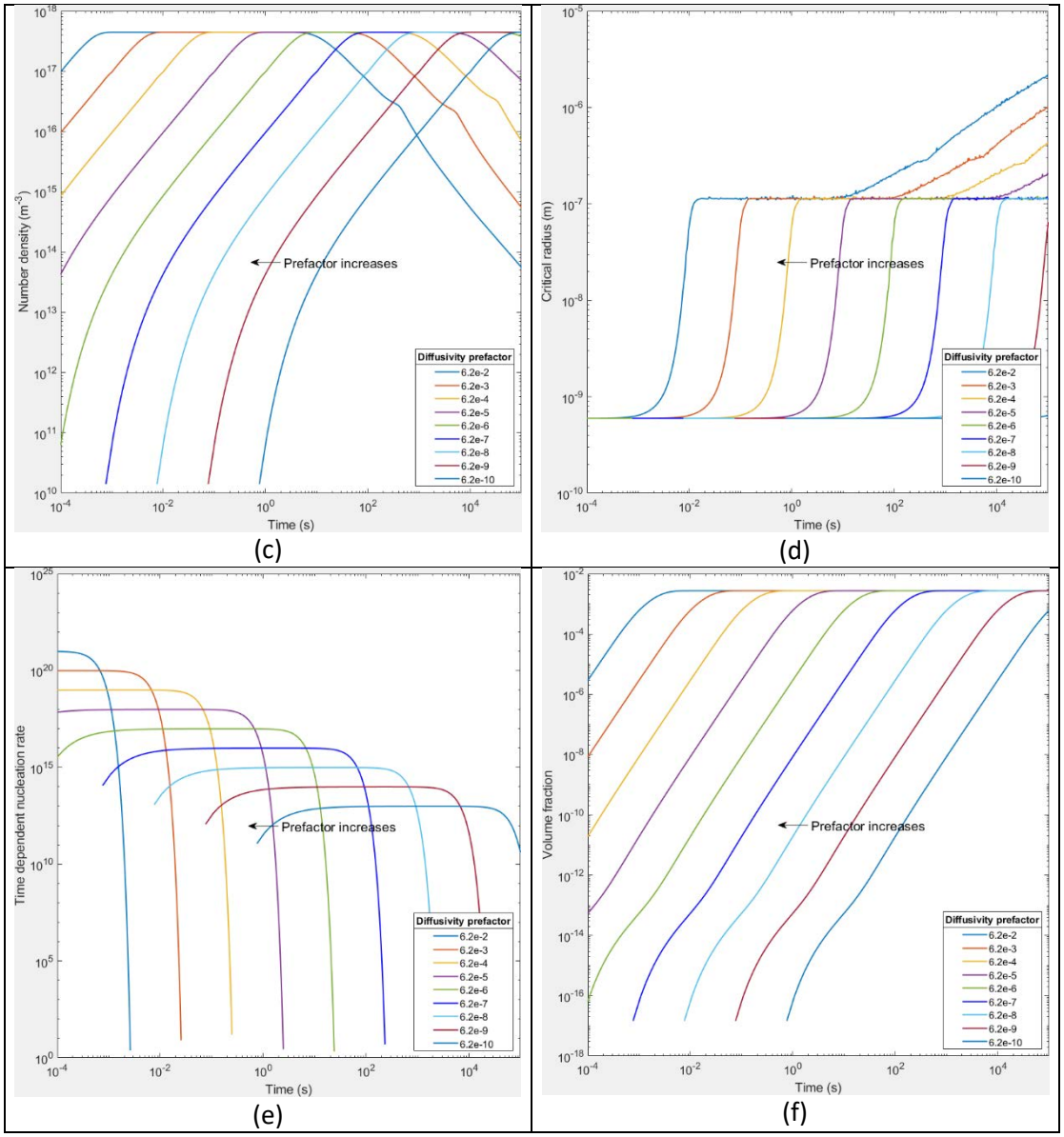

Figure 7: Effect of diffusivity prefactor for (a) composition mass-fraction vs. time, (b) mean radius vs. time, (c) number density vs. time, (d) critical radius vs. time, (e) time dependent nucleation rate vs. time, (f) volume fraction vs. time.

Matrix - Diffusivity Activation Energy

The activation energy was adjusted by orders of magnitude and extra simulations were run for in-between values since a liner correlation was not observed. The observed results indicate that the Diffusivity activation energy is the E_A from the equation:

$$D = D_0 \exp\left(-\frac{E_A}{RT}\right)$$

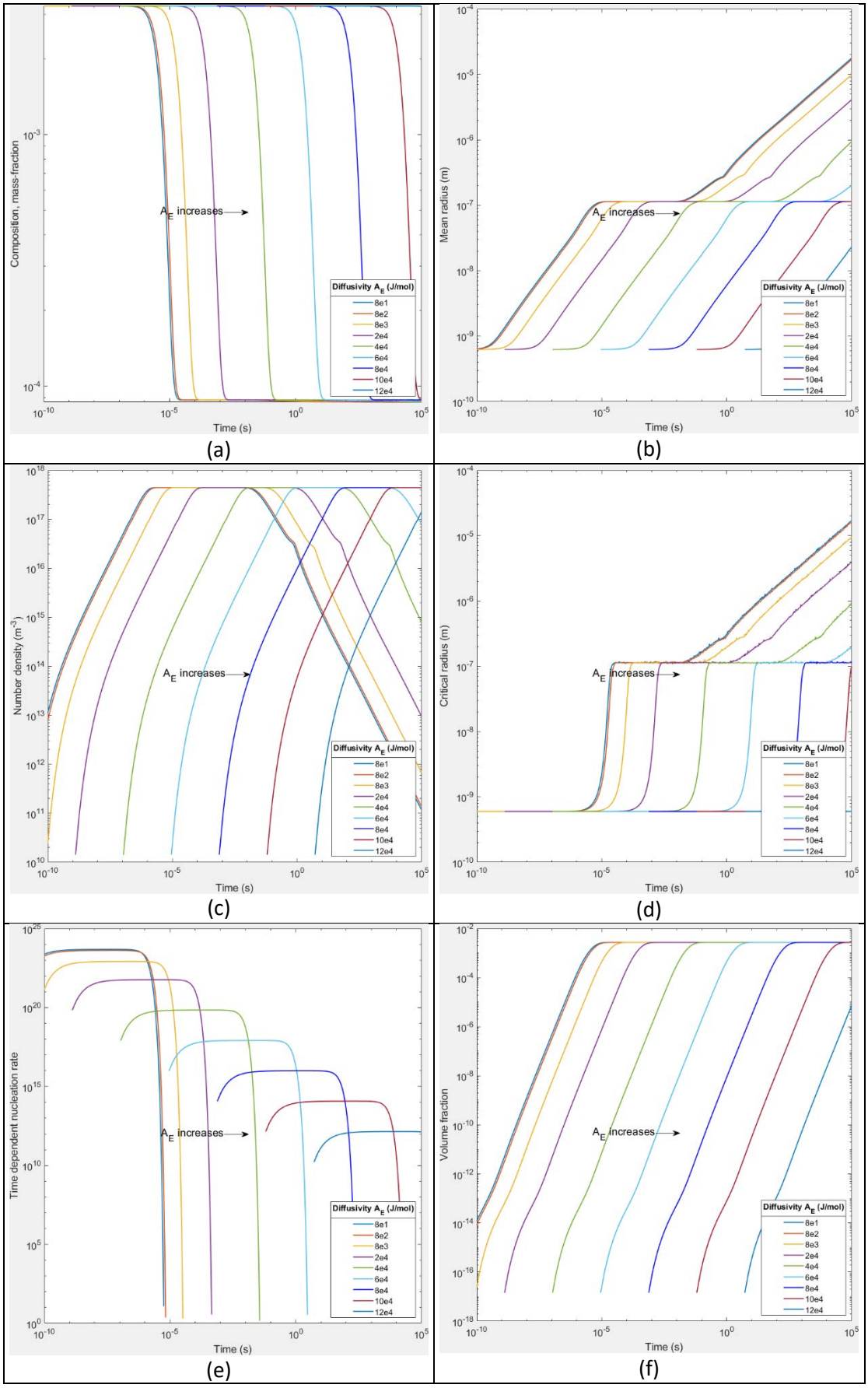

Figure 8: Effect of activation energy of diffusivity for (a) composition mass-fraction vs. time, (b) mean radius vs. time, (c) number density vs. time, (d) critical radius vs. time, (e) time dependent nucleation rate vs. time, (f) volume fraction vs. time.

Precipitate – Interfacial Energy

The interfacial energy for the precipitate phase was adjusted on a smaller scale compared to the previous quantities, since the effect it has on the calculations is of a bigger magnitude as seen from the equation $\Delta G^* = \frac{16\pi\sigma^3}{3\left(\Delta G_m^{\alpha\to\beta} / V_m^{\beta}\right)^2}$.

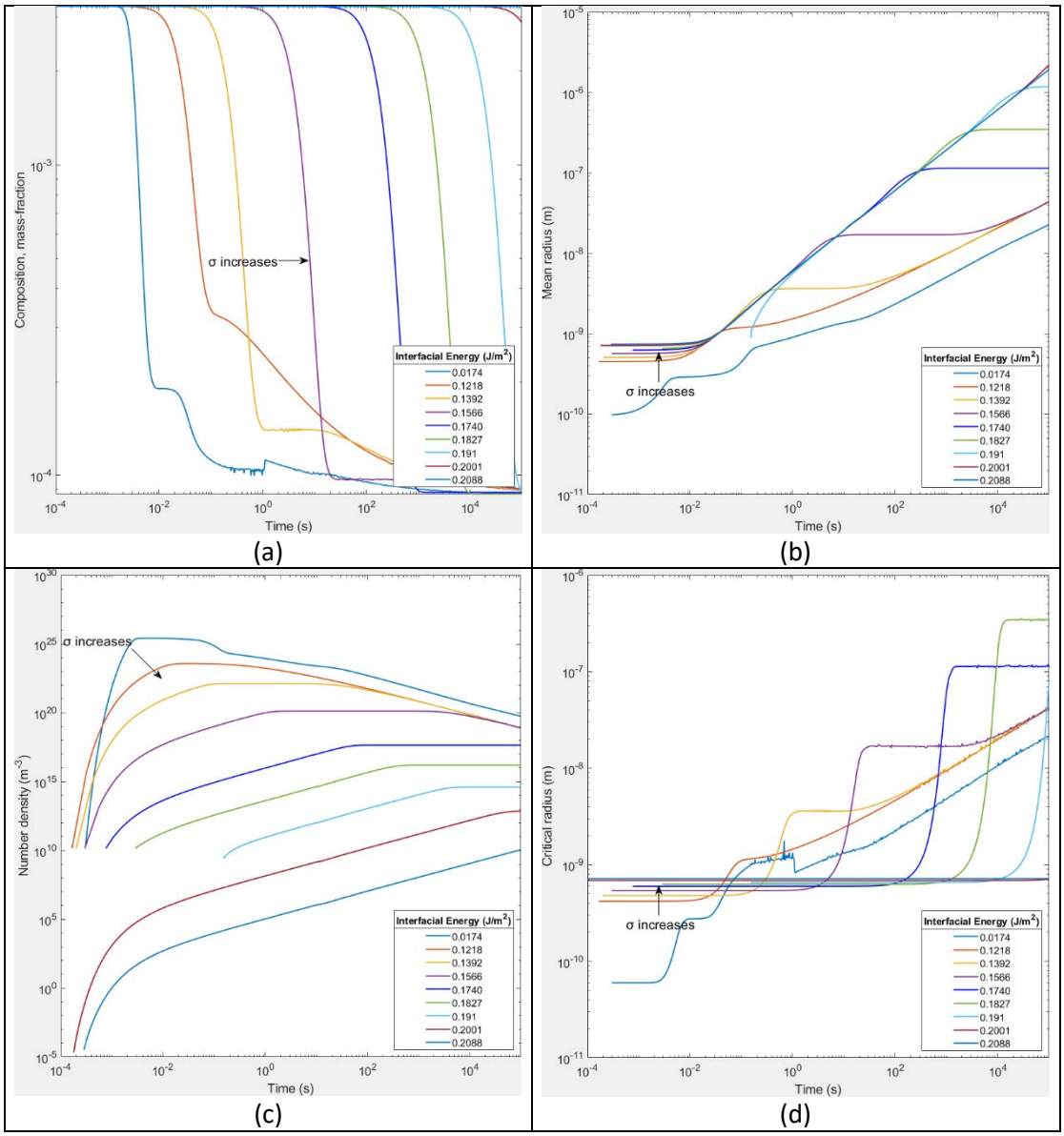

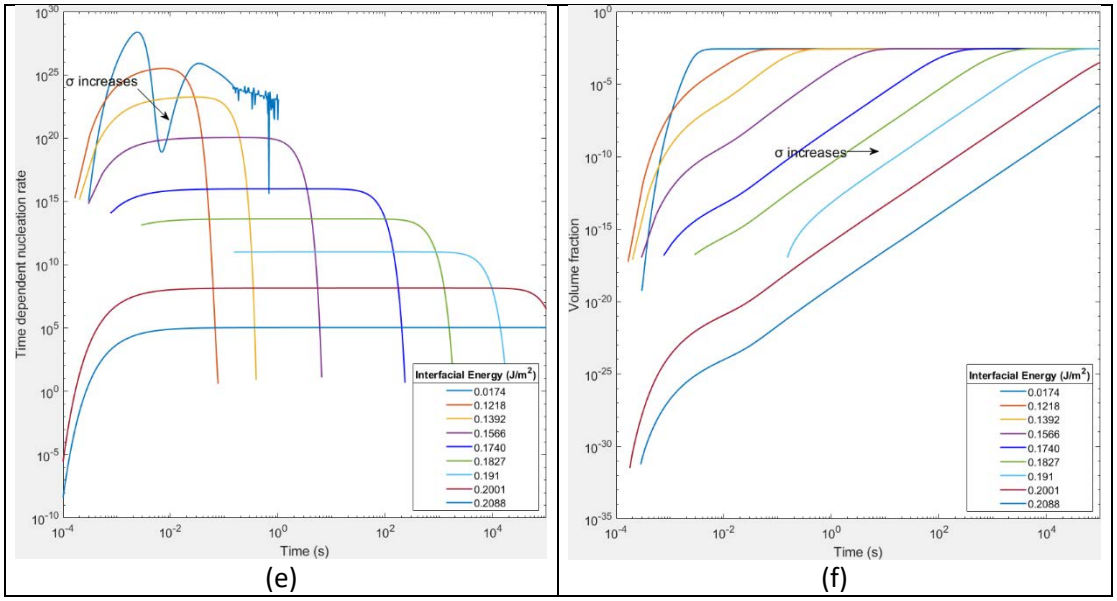

Figure 9: Effect of interfacial energy for (a) composition mass-fraction vs. time, (b) mean radius vs. time, (c) number density vs. time, (d) critical radius vs. time, (e) time dependent nucleation rate vs. time, (f) volume fraction vs. time.

Precipitate – Solvus line Prefactor

A decrease in the solvus line prefactor results in an increased nucleation rate, a smaller mean radius, and a higher number density of precipitates. The maximum volume fraction remains consistent across all cases. Consequently, a lower prefactor yields a finer size distribution of precipitates, while an increase in the prefactor leads to a larger or coarser precipitate distribution.

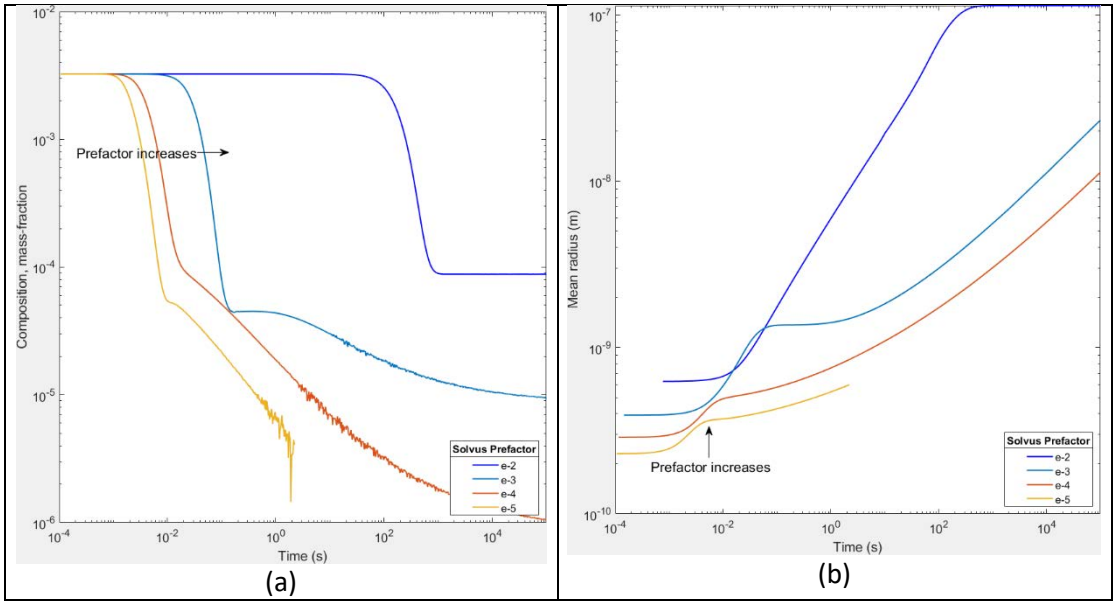

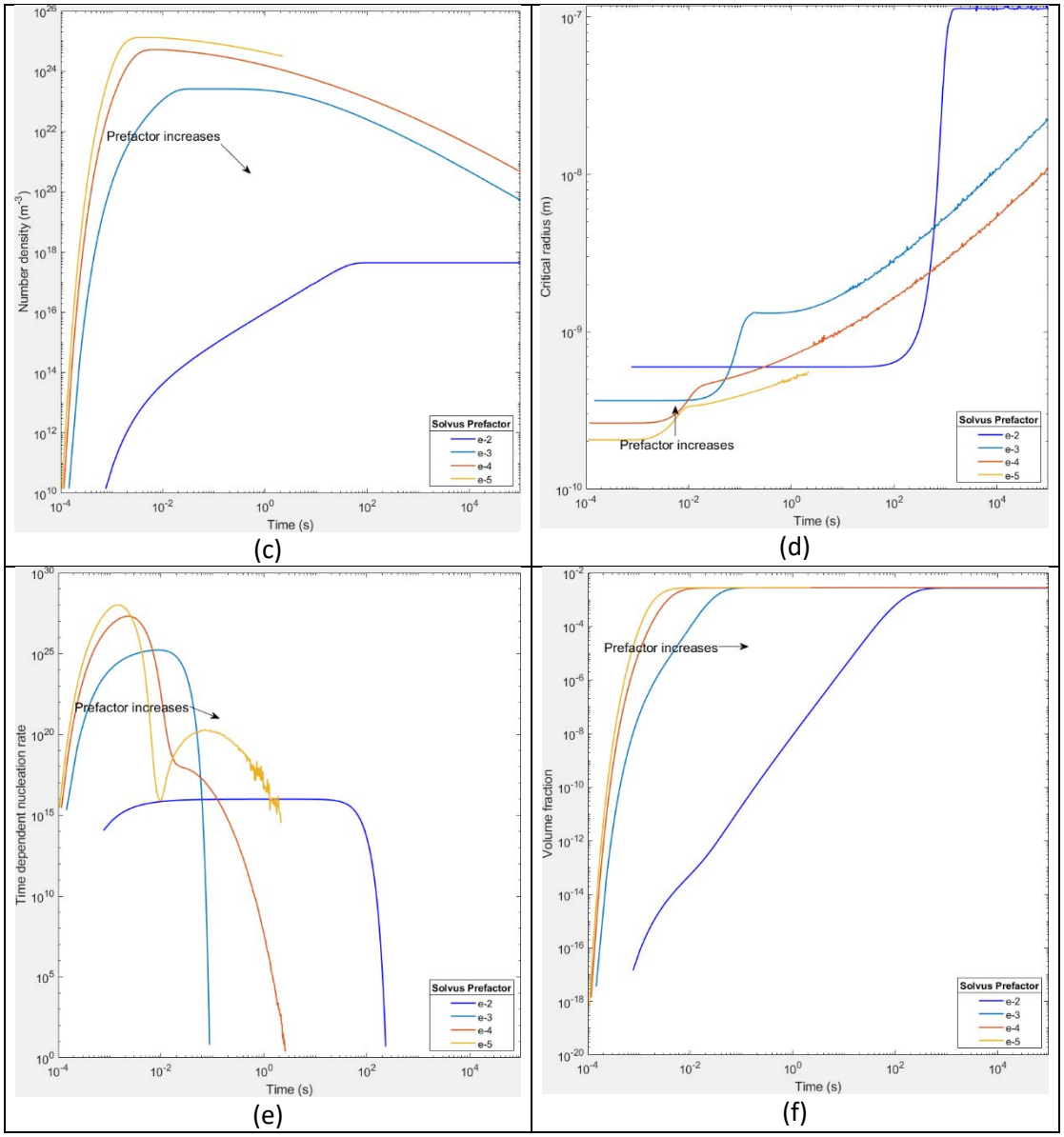

Figure 10: Effect of solvus line prefactor for (a) composition mass-fraction vs. time, (b) mean radius vs. time, (c) number density vs. time, (d) critical radius vs. time, (e) time dependent nucleation rate vs. time, (f) volume fraction vs. time.

Precipitate – Solvus Line Activation Energy

The solvus line activation energy is the energy required for atoms to diffuse and form a solid solution at the solvus line, which delineates the boundary between single-phase and two-phase regions in a phase diagram. This energy is critical in determining the temperature and composition at which a second phase begins to precipitate from a solid solution.

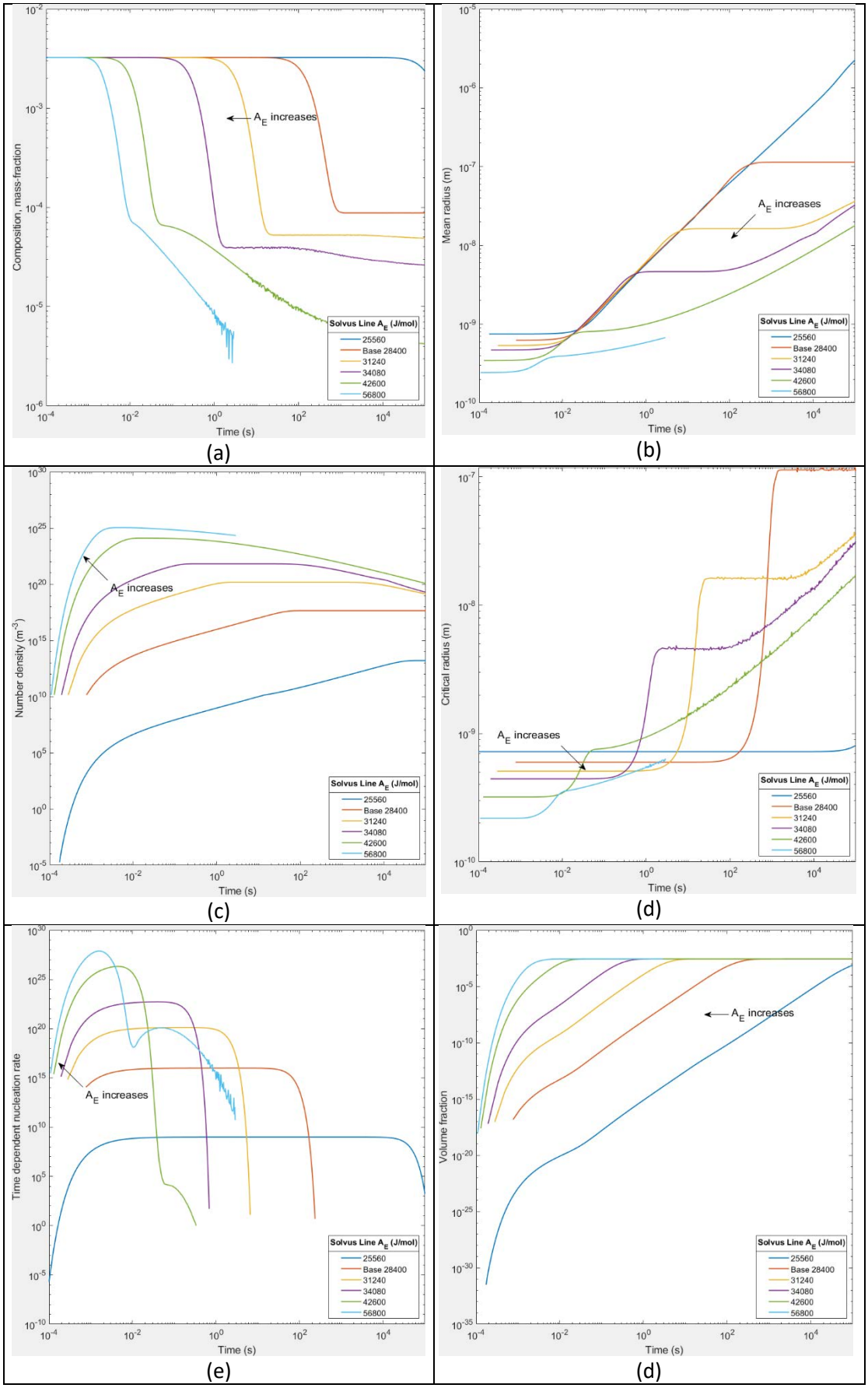

Figure 11: Effect of solvus line activation energy for (a) composition mass-fraction vs. time, (b) mean radius vs. time, (c) number density vs. time, (d) critical radius vs. time, (e) time dependent nucleation rate vs. time, (f) volume fraction vs. time.

The solvus line activation energy significantly influences the kinetics of precipitation. Higher activation energy necessitates more energy for atomic diffusion, thereby slowing down nucleation and growth processes. Conversely, lower activation energy facilitates easier diffusion, promoting faster nucleation and growth of precipitates.

Nb rich carbonitride precipitation

The composition presented in Table 2 from Vervynckt et al. [8] was chosen as reference and then Titanium was removed from the composition as 2 interfering phases were present.

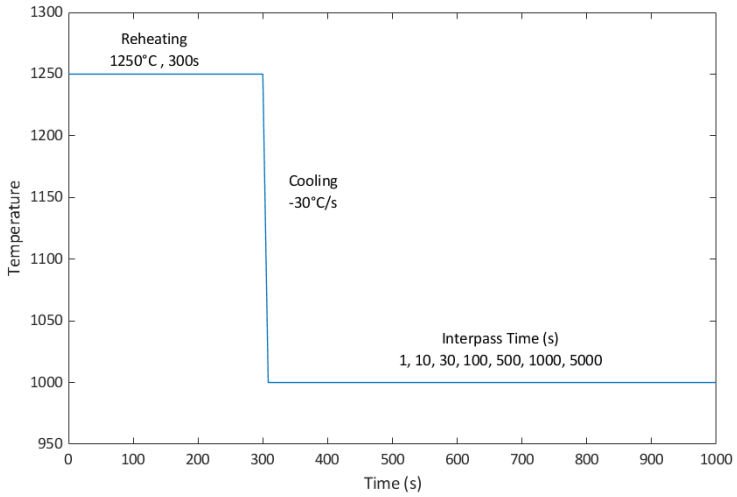

Figure 12: Temperature Profile

The temperature profile was followed and reheating time was removed from the simulation because no nucleation events occurred during this phase, due to a very large nucleation barrier. The first nucleation events take place during the cooling. For the following results, t_0 is the start of the cooling phase, which takes approximately 8.3 seconds. Dislocations were chosen as the nucleation sites; the interfacial energy of the precipitated phase was set at σ_{NbC}=0.5 J/m^2 and the dislocation density at ρ=6.8x10^{13} /m^2.

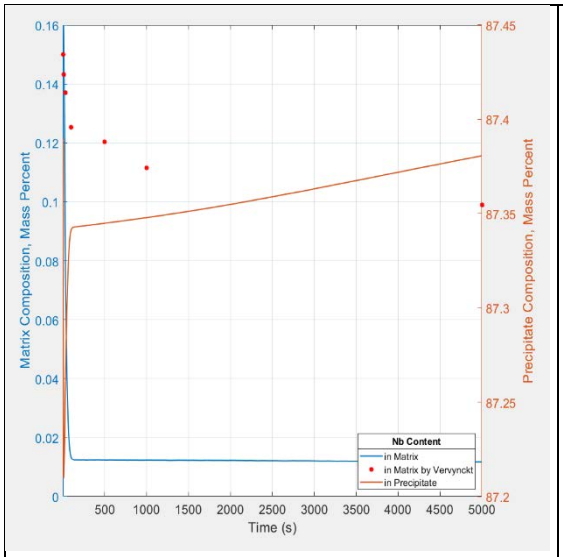

(a)

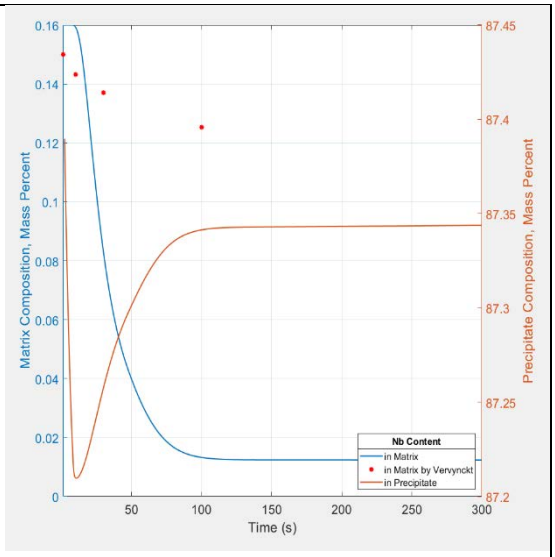

(b)

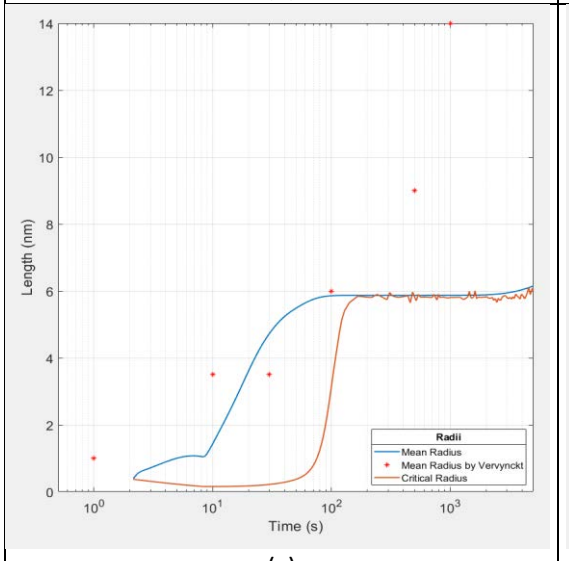

(c)

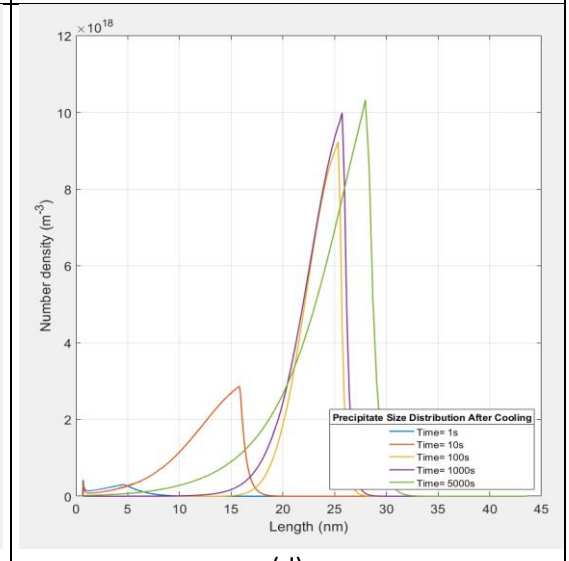

(d)

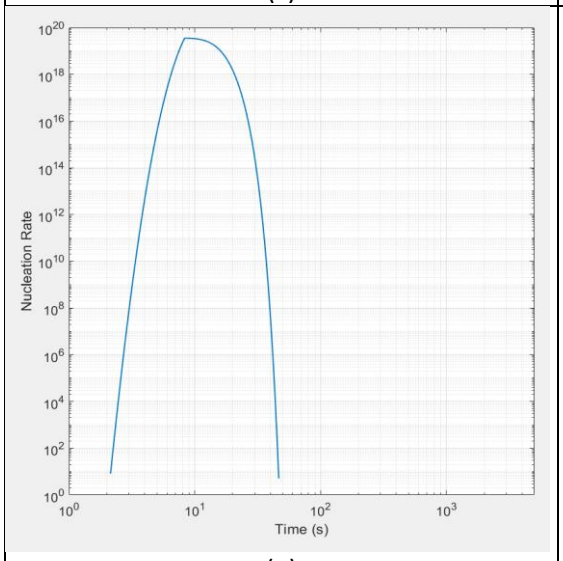

(e)

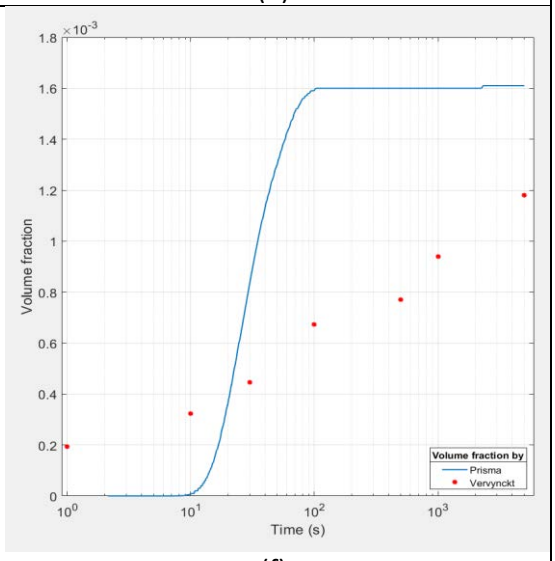

(f)

Figure 13: (a) Nb content in Matrix and Precipitate vs Time, (b) Nb content in Matrix and Precipitate vs Time[1-300s], (c) Mean and Critical radius vs Time, (d) Particle Size Distribution, (e) Nucleation rate vs Time, (f) Volume fraction vs Time

The simulated composition indicates a higher diffusion of Nb into the precipitates compared to the measured values. Specifically, up to 0.15 wt% of Nb was diffused from the matrix in the simulations, whereas Vervynckt's data [8] indicated only 0.061 wt%. Similarly, the volume fraction reaches 0.0016, compared to 0.0011, and does so more rapidly.

The nucleation rate becomes negligible at 45 seconds, after which only the coarsening process is expected to occur. As shown in Fig. 13(c), the mean radius stabilizes at around 6 nm at 100 seconds. The Particle Size Distribution (PSD) curve sharpens and slightly increases in height after 100 seconds, indicating the coarsening of precipitates, where larger precipitates grow at the expense of smaller ones.

These differences arise from the simulation's inability to distinguish between the two phases that can precipitate in the given matrix and temperature. The Ti-rich phase would compete for Nb, thereby retarding the nucleation of the Nb-rich phase. This competition would result in a lower observed volume fraction and Nb content. Even with these differences, the results align with the observed behavior.

4. Conclusions

This study has successfully employed the TC-PRISMA software to approximate the strain-induced precipitation kinetics of Nb carbonitrides in HSLA steels. The parametric analysis conducted on a Fe-C alloy has demonstrated the significant influence of nucleation sites, mobility enhancement factors, and interfacial energy on the nucleation, growth, and coarsening of precipitates. The results indicate that higher nucleation sites and mobility enhancement factors accelerate the precipitation process, while higher activation energy and interfacial energy act as barriers, slowing down the kinetics.

For HSLA steels, the simulations using experimental data from Vervynckt et al. have shown that the processing parameters, such as reheating temperature, cooling rate, and energy and dislocations introduced into the system during the deformation pass, critically affect the precipitation behavior of Nb carbonitrides. The study highlights the importance of precise control over these parameters to achieve the desired microstructure and mechanical properties in HSLA steels [11][12].

Overall, this research provides valuable insights into the strain-induced precipitation of Nb carbonitrides, contributing to the optimization of thermomechanical control processes in HSLA steel production. Future work could focus on further refining the simulation models and exploring the effects of additional alloying elements and complex thermal profiles.

5. Suggestions for future research

The Thermomechanical Control Process will remain a topic of significant interest for both industry and research. The analysis of the carbonitride precipitation plays a crucial role in this area. Further studies can focus on adjusting parameters such as a variable dislocation density to demonstrate the introduction of dislocations during the deformation pass. Additionally, examining a preexisting particle distribution could yield different results.

6. Bibliography / References

[1] Y. Tian, H. Wang, X. Xu, Z. Wang, R. D. K. Misra, and G. Wang, "The Impact of Isothermal Treatment on the Microstructural Evolution and the Precipitation Behavior in High Strength Linepipe Steel," Materials, vol. 13, no. 3, pp. 634–634, Jan. 2020, doi: https://doi.org/10.3390/ma13030634.

[2] J. Górka, "Assessment of Steel Subjected to the Thermomechanical Control Process with Respect to Weldability," Metals, vol. 8, no. 3, p. 169, Mar. 2018, doi: https://doi.org/10.3390/met8030169.

[3] X.-H. Xue, Y.-Y. Shan, L. Zheng, and S.-N. Lou, "Microstructural characteristic of low carbon microalloyed steels produced by thermo-mechanical controlled process," *Materials Science and Engineering A*, vol. 438–440, no. Proceedings of the International Conference on Martensitic Transformations, pp. 285–287, Jun. 2006, doi: https://doi.org/10.1016/j.msea.2006.02.064.

[4] K. Xu, B. G. Thomas, and R. J. O'Malley, "Equilibrium Model of Precipitation in Microalloyed Steels," *Metallurgical and Materials Transactions A*, vol. 42, no. 2, pp. 524–539, Nov. 2010, doi: https://doi.org/10.1007/s11661-010-0428-7.

[5] I. M. Lifshitz and V. V. Slyozov, "The kinetics of precipitation from supersaturated solid solutions," *Journal of Physics and Chemistry of Solids*, vol. 19, no. 1, pp. 35–50, Apr. 1961, doi: https://doi.org/10.1016/0022-3697(61)90054-3.

[6] Wolfgang Pfeiler, *Alloy physics : a comprehensive reference*. Weinheim: Wiley-Vch, 2007, pp. 381–402.

[7] Thermo-Calc Software, "Precipitation Simulations with TC-PRISMA," *Precipitation Module (TC-PRISMA*). https://thermocalc.com/products/add-on-modules/precipitation-module-tc-prisma/

[8] S. Vervynckt, K. Verbeken, Philippe Thibaux, and Yván Houbaert, "Recrystallization–precipitation interaction during austenite hot deformation of a Nb microalloyed steel," *Materials Science and Engineering: A*, vol. 528, no. 16–17, pp. 5519–5528, Jun. 2011, doi: https://doi.org/10.1016/j.msea.2011.03.087.

[9] Thermo-Calc Software, “Precipitation Simulations with TC-PRISMA,” *Precipitation Module (TC-PRISMA)*. https://thermocalc.com/products/add-on-modules/precipitation-module-tc-prisma/

[10] S. Aminorroaya Yamini, “Influence of microalloying elements (Ti, Nb) and nitrogen concentrations on precipitation of pipeline steels—A thermodynamic approach,” *Engineering Reports*, vol. 3, no. 7, Dec. 2020, doi: https://doi.org/10.1002/eng2.12337.

[11] M. Ji, M. Strangwood, and C. Davis, “Effect of Strain-Induced Precipitation on the Recrystallization Kinetics in a Model Alloy,” *Metallurgical and Materials Transactions A*, vol. 52, no. 5, pp. 1963–1975, Mar. 2021, doi: https://doi.org/10.1007/s11661-021-06206-8.

[12] P. Retzl, W. Mayer, D. Krizan, and E. Kozeschnik, “Simulation of Carbo-Nitride Precipitation in the Multi-Phase Microstructure of Micro-Alloyed Transformation-Induced Plasticity Steel,” *steel research international*, vol. 92, no. 1, p. 2000197, Sep. 2020, doi: https://doi.org/10.1002/srin.202000197.